Cell Reports, Volume *36*

Supplemental information

Reprogramming of bivalent chromatin states in *NRAS* mutant melanoma suggests PRC2 inhibition as a therapeutic strategy

Christopher J. Terranova, Ming Tang, Mayinuer Maitituoheti, Ayush T. Raman, Archit K. Ghosh, Jonathan Schulz, Samir B. Amin, Elias Orouji, Katarzyna Tomczak, Sharmistha Sarkar, Junna Oba, Caitlin Creasy, Chang-Jiun Wu, Samia Khan, Rossana Lazcano, Khalida Wani, Anand Singh, Praveen Barrodia, Dongyu Zhao, Kaifu Chen, Lauren E. Haydu, Wei-Lien Wang, Alexander J. Lazar, Scott E. Woodman, Chantale Bernatchez, and Kunal Rai

Figure S1

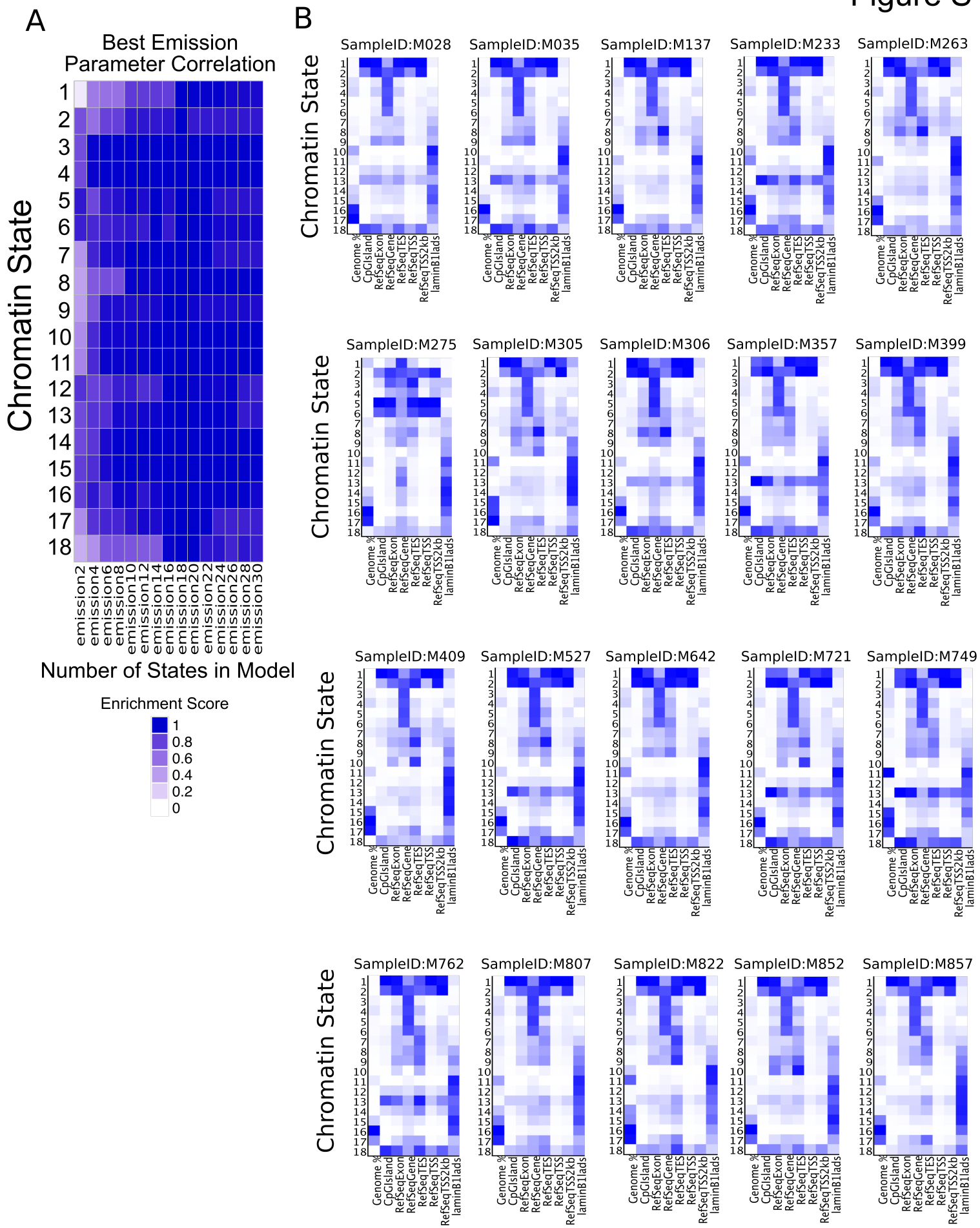
A
Best Emission Parameter Correlation
Chromatin State
1
2
3
4
5
6
7
8
9
10
11
12
13
14
15
16
17
18
emission2
emission4
emission6
emission8
emission10
emission12
emission14
emission16
emission18
emission20
emission22
emission24
emission26
emission28
emission30
Number of States in Model
Enrichment Score
1
0.8
0.6
0.4
0.2
0
B
SampleID:M028
SampleID:M035
SampleID:M137
SampleID:M233
SampleID:M263
SampleID:M275
SampleID:M305
SampleID:M306
SampleID:M357
SampleID:M399
SampleID:M409
SampleID:M527
SampleID:M642
SampleID:M721
SampleID:M749
SampleID:M762
SampleID:M807
SampleID:M822
SampleID:M852
SampleID:M857
Chromatin State
Genome %
CpGIsland
RefSeqExon
RefSeqGene
RefSeqTES
RefSeqTSS
RefSeqTSS2kb
laminB1lads

SUPPLEMENTAL FIGURE LEGENDS:

Figure S1: Representative chromatin state probabilities for melanoma tumors. Related to Figure 1 and Table S1.
A) Emission parameter correlation plot comparing the 18-state model used in this study and chromatin models between 2-30 states in 20 metastatic melanoma tumors samples from TCGA.
B) Genomic annotation enrichments for each chromatin state in 20 metastatic melanoma tumor samples from TCGA.

Figure S2

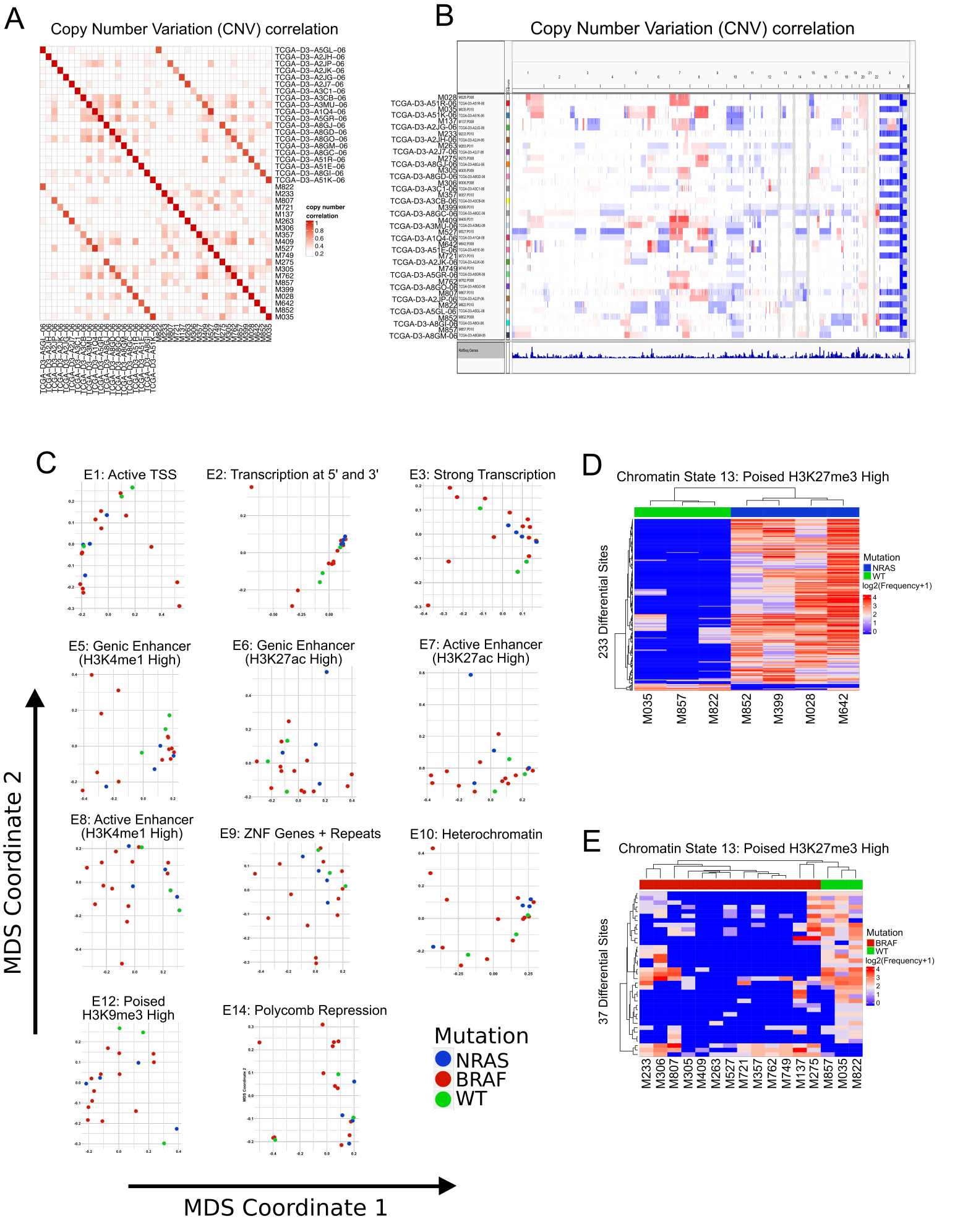
A
Copy Number Variation (CNV) correlation
copy number correlation
B
Copy Number Variation (CNV) correlation
C
E1: Active TSS
E2: Transcription at 5' and 3'
E3: Strong Transcription
E5: Genic Enhancer (H3K4me1 High)
E6: Genic Enhancer (H3K27ac High)
E7: Active Enhancer (H3K27ac High)
E8: Active Enhancer (H3K4me1 High)
E9: ZNF Genes + Repeats
E10: Heterochromatin
E12: Poised H3K9me3 High
E14: Polycomb Repression
MDS Coordinate 2
MDS Coordinate 1
Mutation
NRAS
BRAF
WT
D
Chromatin State 13: Poised H3K27me3 High
233 Differential Sites
Mutation
NRAS
WT
log2(Frequency+1)
M035
M857
M822
M852
M399
M028
M642
E
Chromatin State 13: Poised H3K27me3 High
37 Differential Sites
Mutation
BRAF
WT
log2(Frequency+1)
M233
M306
M807
M305
M409
M263
M527
M721
M357
M762
M749
M137
M275
M857
M035
M822

Figure S2: Combinatorial chromatin states and copy number variation correlation for melanoma tumors; MDS and heatmap analysis of chromatin states annotated by mutational subtype. Related to Figure 1 and Table S1.

A) Copy Number Variation (CNV) correlation between the 20 melanoma tumors profiled and CNV classification from TCGA based on all genes.

B) Genome browser view of CNV correlation between the 20 melanoma tumors profiled and CNV classification from TCGA.

C) MDS analysis of chromatin states from 20 metastatic melanoma tumors annotated by mutation (NRAS, BRAF, WT) based on TCGA classification.

D) Heatmap displaying differentially regulated regions (FDR < 0.05) of chromatin state 13 (poised H3K27me3 high) between *NRAS* and WT tumor subtypes.

E) Heatmap displaying differentially regulated regions (FDR < 0.05) of chromatin state 13 (poised H3K27me3 high) between *BRAF* and WT tumor subtypes.

Figure S3

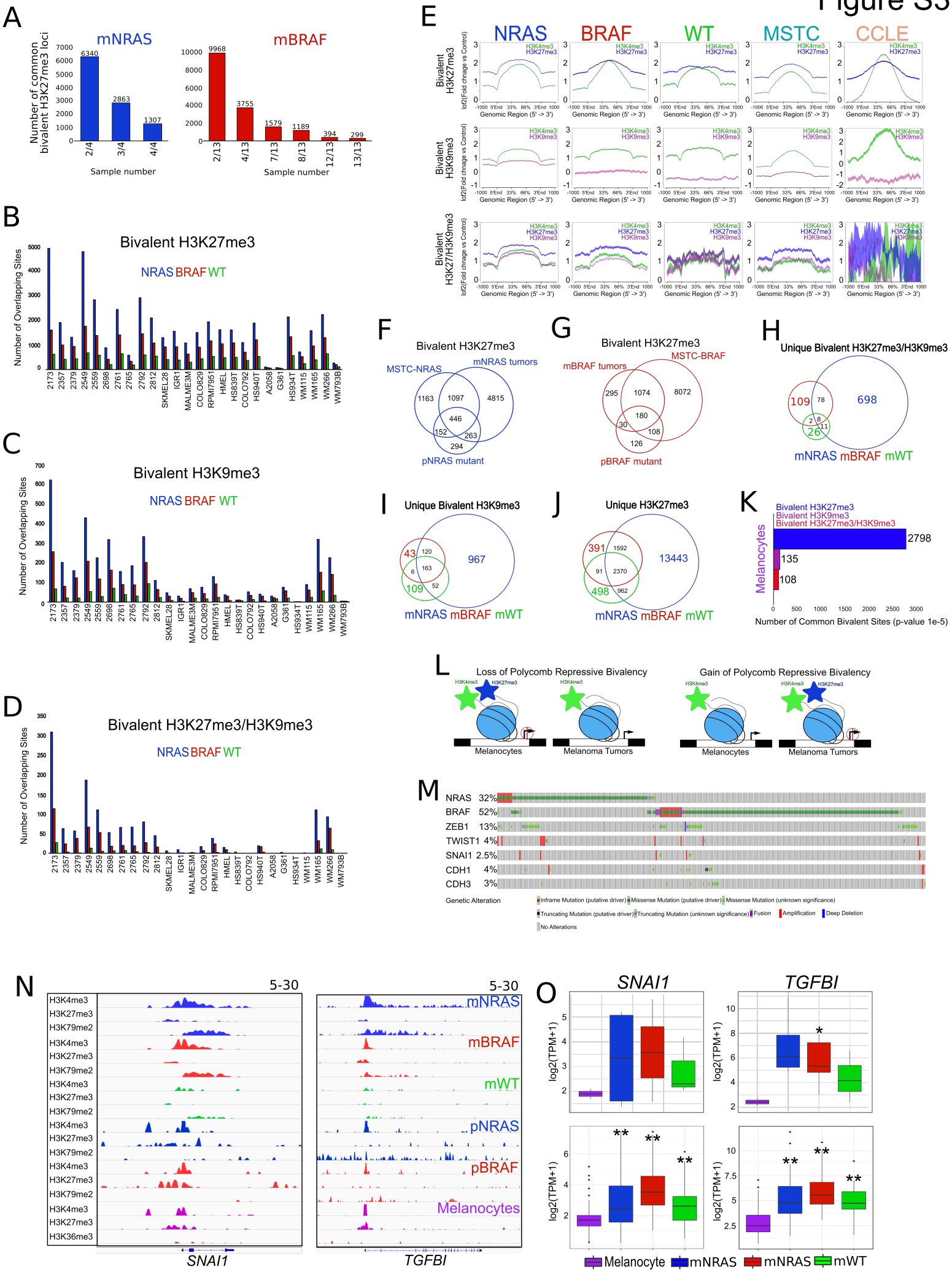
A
mNRAS
mBRAF
Number of common bivalent H3K27me3 loci
Sample number
2/4
3/4
4/4
2/13
4/13
7/13
8/13
12/13
13/13
B
Bivalent H3K27me3
NRAS BRAF WT
Number of Overlapping Sites
C
Bivalent H3K9me3
NRAS BRAF WT
D
Bivalent H3K27me3/H3K9me3
NRAS BRAF WT
E
NRAS
BRAF
WT
MSTC
CCLE
Bivalent H3K27me3
Bivalent H3K9me3
Bivalent H3K27/H3K9me3
Genomic Region (5' -> 3')
F
Bivalent H3K27me3
MSTC-NRAS
mNRAS tumors
pNRAS mutant
G
Bivalent H3K27me3
mBRAF tumors
MSTC-BRAF
pBRAF mutant
H
Unique Bivalent H3K27me3/H3K9me3
mNRAS mBRAF mWT
I
Unique Bivalent H3K9me3
mNRAS mBRAF mWT
J
Unique H3K27me3
mNRAS mBRAF mWT
K
Bivalent H3K27me3
Bivalent H3K9me3
Bivalent H3K27me3/H3K9me3
Melanocytes
Number of Common Bivalent Sites (p-value 1e-5)
L
Loss of Polycomb Repressive Bivalency
Gain of Polycomb Repressive Bivalency
Melanocytes
Melanoma Tumors
M
NRAS 32%
BRAF 52%
ZEB1 13%
TWIST1 4%
SNAI1 2.5%
CDH1 4%
CDH3 3%
Genetic Alteration
Inframe Mutation (putative driver)
Missense Mutation (putative driver)
Missense Mutation (unknown significance)
Truncating Mutation (putative driver)
Truncating Mutation (unknown significance)
Fusion
Amplification
Deep Deletion
No Alterations
N
5-30
H3K4me3
H3K27me3
H3K79me2
H3K36me3
mNRAS
mBRAF
mWT
pNRAS
pBRAF
Melanocytes
SNAI1
TGFBI
O
SNAI1
TGFBI
log2(TPM+1)
Melanocyte
mNRAS
mNRAS
mWT

Figure S3: Genome-wide analysis of bivalent H3K27me3 and H3K9me3 associated loci. Related to Figure 1, Figure 2 and Table S2.

A) Number of common bivalent H3K27me3 associated loci in *NRAS*- and *BRAF*- mutant tumors.

B) Co-occupancy analysis of common bivalent H3K27me3 associated loci in melanoma tumor subtypes directly overlapping bivalent H3K27me3 associated loci in individual MSTC or CCLE lines.

C) Co-occupancy analysis of common bivalent H3K9me3 associated loci in melanoma tumor subtypes directly overlapping bivalent H3K9me3 associated loci in individual MSTC or CCLE lines.

D) Co-occupancy analysis of common bivalent H3K27/H3K9me3 associated loci in melanoma tumor subtypes directly overlapping total bivalent H3K27/H3K9me3 associated loci in individual MSTC or CCLE lines.

E) Average density profiles of common bivalent H3K27me3, bivalent H3K9me3 and bivalent H3K27/H3K9me3 loci in melanoma tumor subtypes, MSTC and CCLE lines.

F) Venn diagram analysis of bivalent H3K27me3 associated loci in *NRAS*-mutant melanoma tumors (mNRAS), *NRAS*-mutant MSTC (MSTC-2125, MSTC-2770, MSTC-2495) and pNRAS isogenic mutant melanocytes.

G) Venn diagram analysis of bivalent H3K27me3 associated loci in *BRAF*-mutant melanoma tumors (mBRAF), *BRAF*-mutant MSTC (MSTC-2549, MSTC-2765, MSTC-2357) and pBRAF isogenic mutant melanocytes.

H-J) Venn diagram analysis of bivalent H3K27me3/H3K9me3, I) bivalent H3K9me3 and J) polycomb H3K27me3 associated loci in melanoma tumor subtypes.

K) Common bivalent H3K27me3, bivalent H3K9me3 and bivalent H3K27/H3K9me3 associated loci in primary melanocytes from Roadmap. Associated loci were identified as common if they were present in 2/2 melanocytes.

L) Schematic of bivalent H3K27me3 associated losses and gains between melanocytes and melanoma tumors.

M) OncoPrint of all possible genetic alterations in *NRAS*, *BRAF*, *ZEB1*, *TWIST1*, *SNAI1*, *CDH1* and *CHD3* genes from 363 skin cutaneous melanoma samples.

N) Genome browser view of ChIP-seq tracks for H3K4me3, H3K27me3 and active transcription (H3K79me2/H3K36me3) on the *SNAI1* and *TGFBI* genes in mNRAS, mBRAF, mWT melanoma tumor subtypes, isogenic mutant melanocytes and primary melanocytes from Roadmap.

O) Boxplot displaying quantile normalized mean RNA-expression profiles (log2 TPM) of the *SNAI1* and *TGFBI* genes in melanocytes (n=2) and melanoma tumor subtypes (NRAS=4, BRAF=13, WT=3) with associated chromatin profiles (top) and in a large cohort of melanocytes (n= 86) and melanoma tumor subtypes (NRAS=81, BRAF=118, WT=38 (bottom)). P-values were calculated using a wilcoxon test. * = p-value < 0.05; ** = p-value <0.0001.

Figure S4

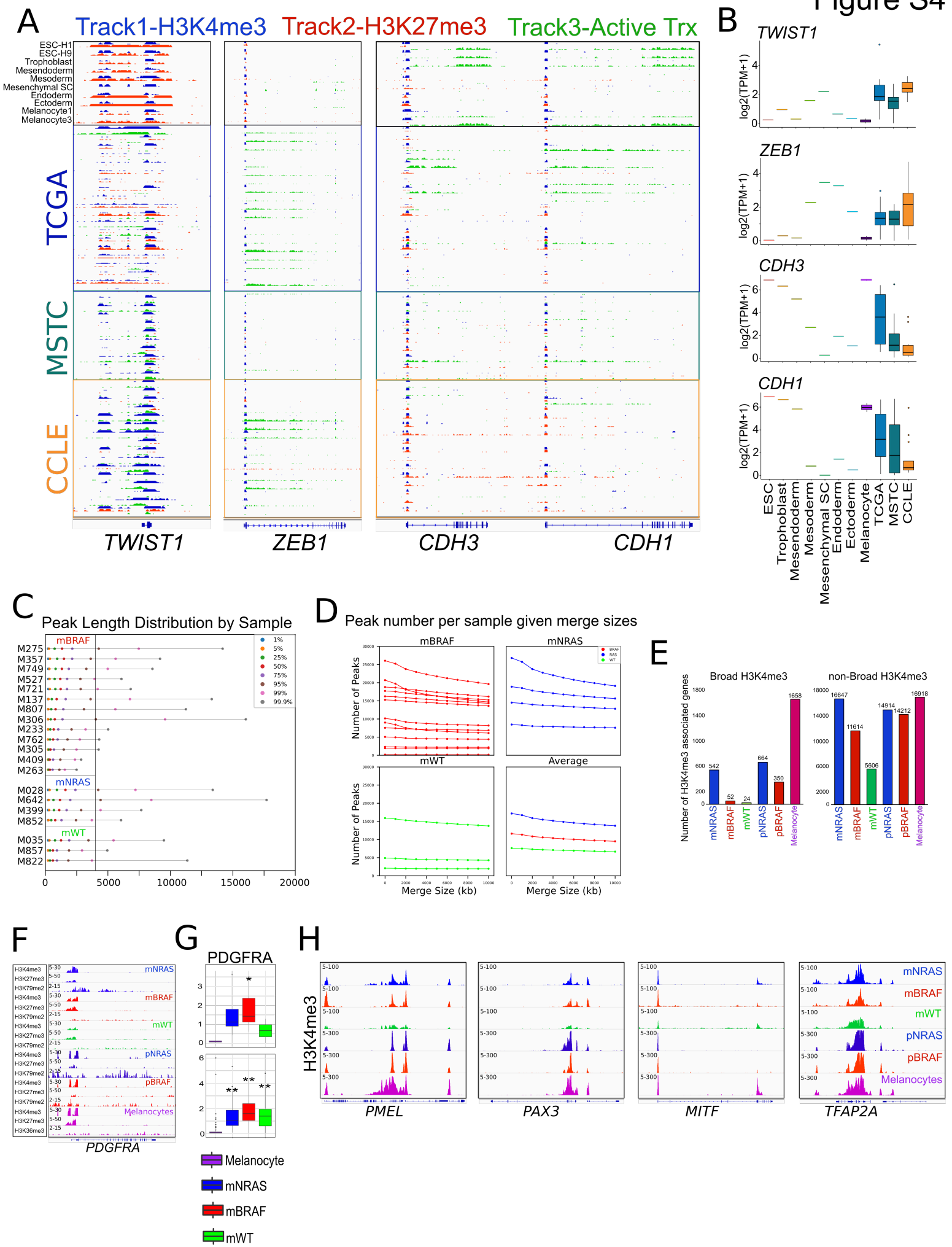
A
Track1-H3K4me3
Track2-H3K27me3
Track3-Active Trx
ESC-H1
ESC-H9
Trophoblast
Mesendoderm
Mesoderm
Mesenchymal SC
Endoderm
Ectoderm
Melanocyte1
Melanocyte3
TCGA
MSTC
CCLE
TWIST1
ZEB1
CDH3
CDH1
B
TWIST1
ZEB1
CDH3
CDH1
log2(TPM+1)
ESC
Trophoblast
Mesendoderm
Mesoderm
Mesenchymal SC
Endoderm
Ectoderm
Melanocyte
TCGA
MSTC
CCLE
C
Peak Length Distribution by Sample
mBRAF
mNRAS
mWT
1%
5%
25%
50%
75%
95%
99%
99.9%
M275
M357
M749
M527
M721
M137
M807
M306
M233
M762
M305
M409
M263
M028
M642
M399
M852
M035
M857
M822
0
5000
10000
15000
20000
D
Peak number per sample given merge sizes
mBRAF
mNRAS
mWT
Average
Number of Peaks
Merge Size (kb)
E
Broad H3K4me3
non-Broad H3K4me3
Number of H3K4me3 associated genes
542
52
24
664
350
1658
16647
11614
5606
14914
14212
16918
mNRAS
mBRAF
mWT
pNRAS
pBRAF
Melanocyte
F
mNRAS
mBRAF
mWT
pNRAS
pBRAF
Melanocytes
PDGFRA
G
PDGFRA
Melanocyte
mNRAS
mBRAF
mWT
H
H3K4me3
PMEL
PAX3
MITF
TFAP2A
mNRAS
mBRAF
mWT
pNRAS
pBRAF
Melanocytes

Figure S4: EMT-TF genes gain and lose bivalent domains during melanoma progression; Broad H3K4me3 domains as an epigenetic feature in metastatic melanoma. Related to Figure 2, Figure 3, Figure 4, Table S3, Table S4 and Table S5.

A) Genome browser view of ChIP-seq tracks for H3K4me3, H3K27me3 and active transcription (H3K79me2/H3K36me3) on the *TWIST1*, *ZEB1*, *CDH3* and *CDH3* genes in ESC, Trophoblast, Mesendoderm, Mesoderm, Mesenchymal Stem Cells, Endoderm, Ectoderm, melanocytes from Roadmap and TCGA tumors, MSTC and CCLE cell lines.

B) Boxplots displaying quantile normalized mean RNA-expression profiles (log2 TPM) of the *TWIST1*, *ZEB1*, *CDH3* and *CDH3* genes in ESC, Trophoblast, Mesendoderm, Mesoderm, Mesenchymal Stem Cells, Endoderm, Ectoderm, melanocytes from Roadmap and TCGA tumors, MSTC and CCLE cell lines.

C) Quartile plot displaying peak length distribution based on percentage of broadest H3K4me3 domains in mBRAF, mNRAS and mWT melanoma tumors. Black line denotes 4kb peak length.

D) LinePlot displaying total H3K4me3 peak number at merge sizes between 1kb to 10kb in mBRAF, mNRAS and mWT samples. Bottom right plot displays average by mutational subtype.

E) Barplot of broad H3K4me3 (> 4kb) and non-broad H3K4me3 (< 4kb) domains in mNRAS, mBRAF, mWT melanoma tumor subtypes, isogenic mutant melanocytes and primary melanocytes from Roadmap.

F) Genome browser view of ChIP-seq tracks for H3K4me3, H3K27me3 and active transcription (H3K79me2/H3K36me3) on the *PDGFRA* gene in mNRAS, mBRAF, mWT melanoma tumor subtypes, isogenic mutant melanocytes and primary melanocytes from Roadmap.

G) Boxplot displaying quantile normalized mean RNA-expression profiles (log2 TPM) of the PDGFRA gene in melanocytes (n=2) and melanoma tumor subtypes (NRAS=4, BRAF=13, WT=3) with associated chromatin profiles (top) and in a large cohort of melanocytes (n= 86) and melanoma tumor subtypes (NRAS=81, BRAF=118, WT=38 (bottom)). P-values were calculated using a wilcoxon test. * = p-value < 0.05; ** = p-value <0.0001.

H) Genome browser view of ChIP-seq tracks displaying H3K4me3 on the *PMEL*, *PAX3*, *MITF* and *TFAP2A* genes in mNRAS, mBRAF, mWT melanoma tumor subtypes, isogenic mutant melanocytes and primary melanocytes from Roadmap.

Figure S5

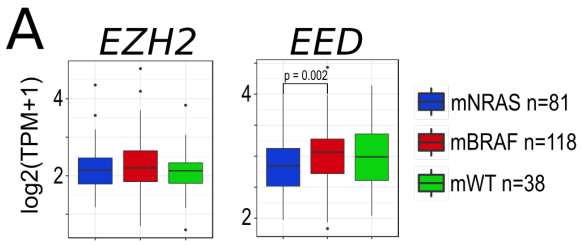
A
EZH2
EED
log2(TPM+1)
p = 0.002
mNRAS n=81
mBRAF n=118
mWT n=38

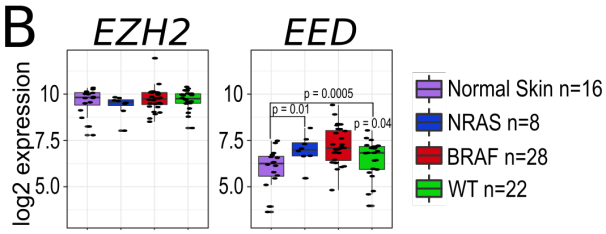
B
EZH2
EED
log2 expression
p = 0.01
p = 0.0005
p = 0.04
Normal Skin n=16
NRAS n=8
BRAF n=28
WT n=22

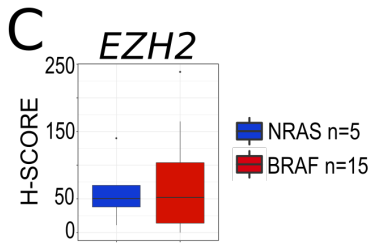
C
EZH2
H-SCORE
NRAS n=5
BRAF n=15

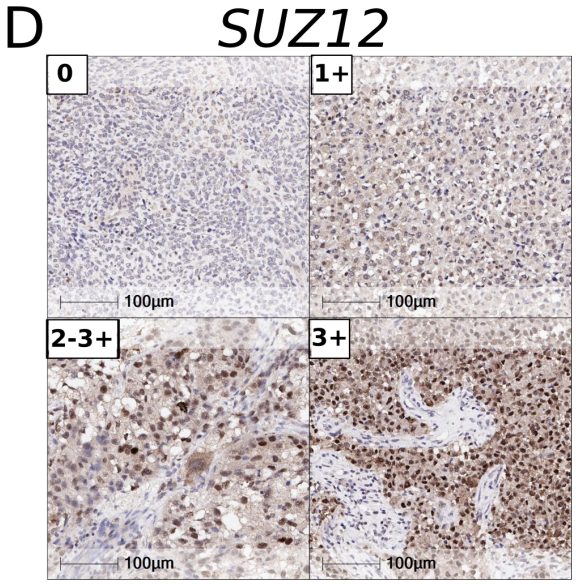
D
SUZ12
0
1+
2-3+
3+
100µm

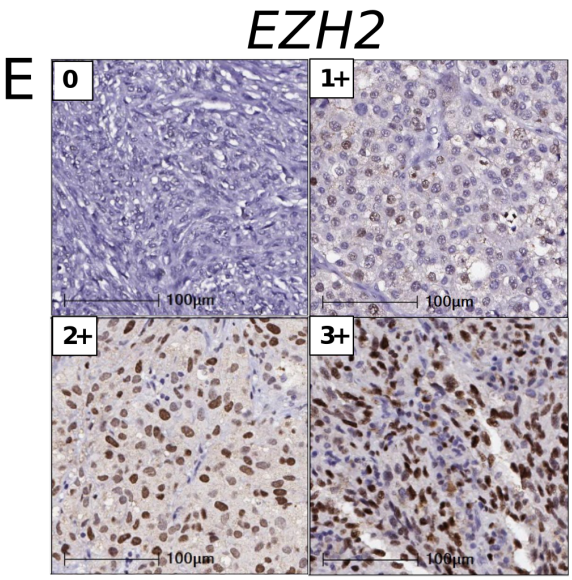
E
EZH2
0
1+
2+
3+
100µm

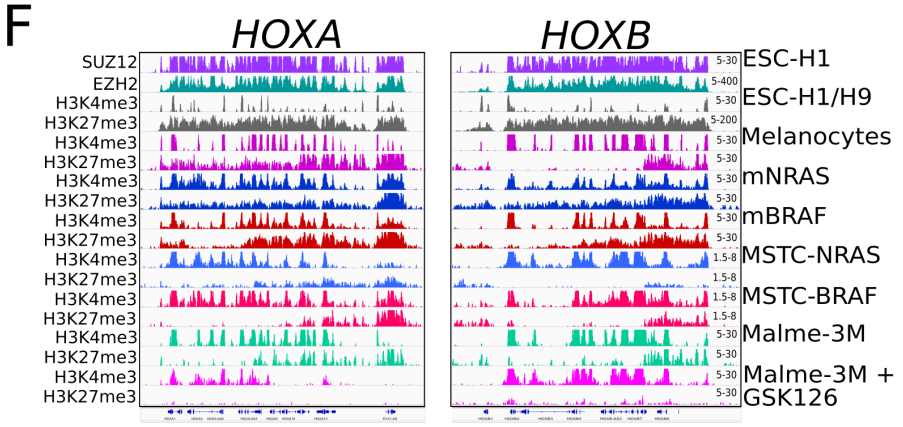
F
HOXA
HOXB
SUZ12
EZH2
H3K4me3
H3K27me3
ESC-H1
ESC-H1/H9
Melanocytes
mNRAS
mBRAF
MSTC-NRAS
MSTC-BRAF
Malme-3M
Malme-3M + GSK126

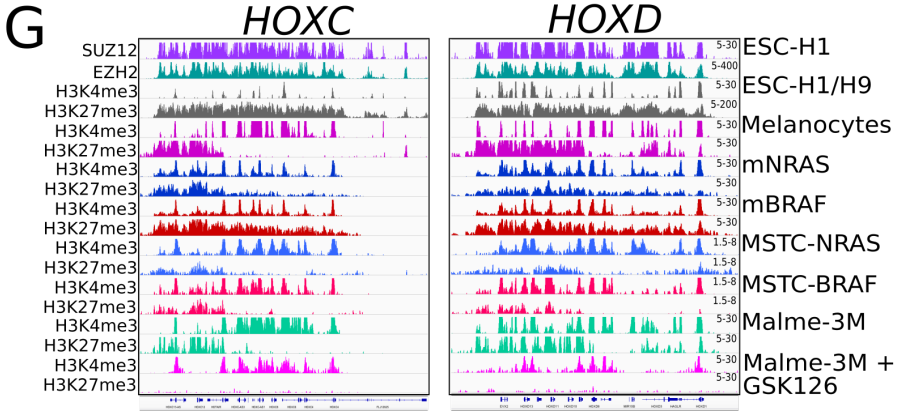
G
HOXC
HOXD
SUZ12
EZH2
H3K4me3
H3K27me3
ESC-H1
ESC-H1/H9
Melanocytes
mNRAS
mBRAF
MSTC-NRAS
MSTC-BRAF
Malme-3M
Malme-3M + GSK126

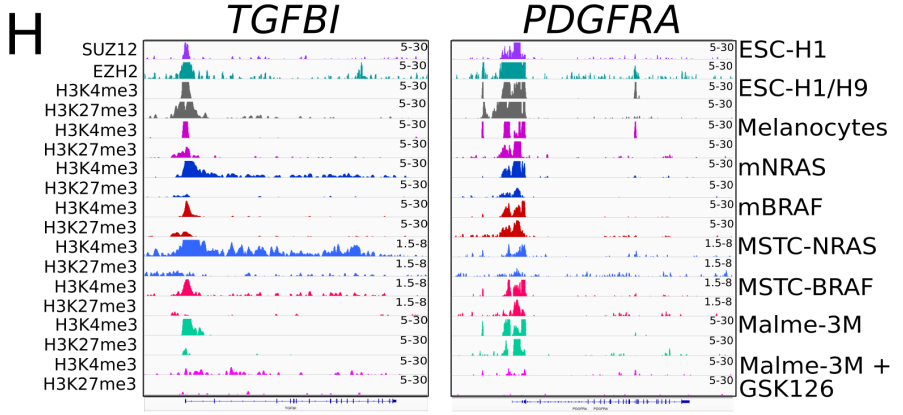
H
TGFBI
PDGFRA
SUZ12
EZH2
H3K4me3
H3K27me3
ESC-H1
ESC-H1/H9
Melanocytes
mNRAS
mBRAF
MSTC-NRAS
MSTC-BRAF
Malme-3M
Malme-3M + GSK126

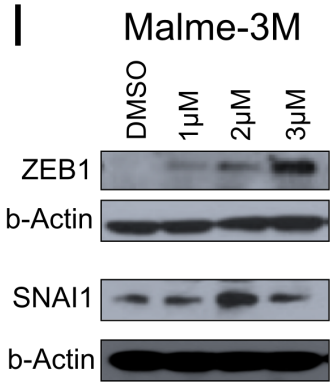
I
Malme-3M
DMSO
1µM
2µM
3µM
ZEB1
b-Actin
SNAI1
b-Actin

Figure S5: PRC2 is expressed in *NRAS*-mutant melanomas. Related to Figure 5.
A) Boxplot displaying quantile normalized mean RNA-expression profiles (log2 TPM) for the *EZH2* and *EED* genes in melanoma tumor subtypes (NRAS=81, BRAF=118, WT=38) from the TCGA dataset.
B) Boxplot displaying microarray profiles (log2) in normal skin and melanoma tumors for the *EZH2* and *EED* genes from the GSE15605 dataset.
C) Boxplot displaying H-SCORES from EZH2 immunohistochemistry staining in patient TMA harboring an *NRAS*-mutation (patients = 5; samples = 10) or *BRAF*-mutation (patients = 15; samples = 31). P-values were calculated using a t-test based on H-SCORES in each mutational subtype.
D) Representative images from immunohistochemistry staining for SUZ12 in patient TMA. Scale bar represent 100μM.
E) Representative images from immunohistochemistry staining for EZH2 in patient TMA. Scale bar represent 100μM.
F-H) Genome browser view of ChIP-seq tracks for SUZ12, EZH2, H3K4me3 and H3K27me3 in ESCs, and H3K4me3 and H3K27me3 in melanocytes, mNRAS and mBRAF tumors, representative *NRAS*-mutant MSTC (MSTC-2125, MSTC-2770, MSTC-2495), *BRAF*-mutant MSTC (MSTC-2549, MSTC-2765, MSTC-2357), and in Malme-3M cells treated for 14 days with GSK-126 or DMSO on the F-G) *HOX* cluster genes and H) EMT-TF genes *TGFBI* and *PDGFRA*.
I) Western blotting analysis for ZEB1 and SNAI1 in Malme-3M cells treated for 14 days with GSK-126 or DMSO.

Figure S6

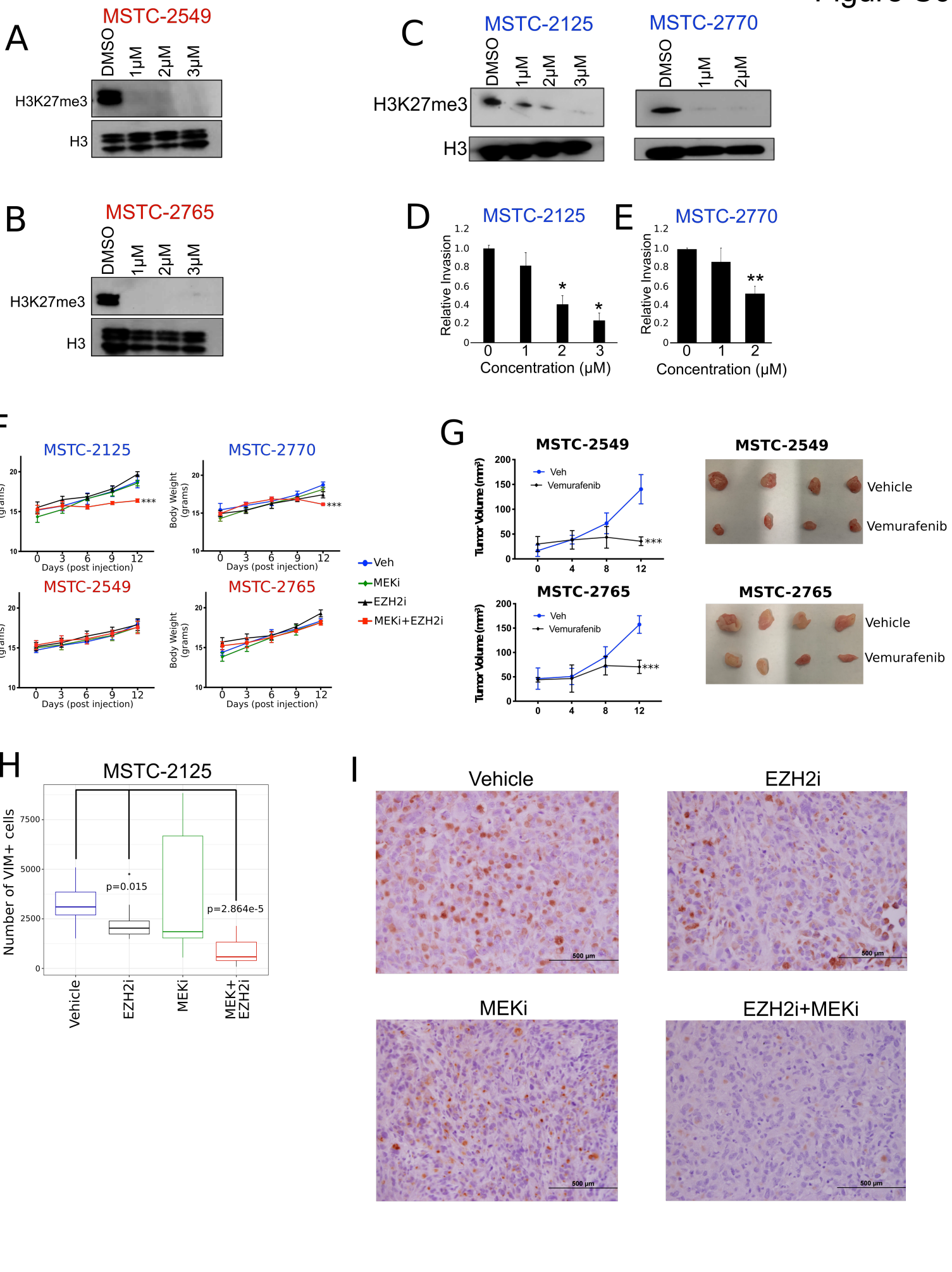
A
MSTC-2549
DMSO
1μM
2μM
3μM
H3K27me3
H3
B
MSTC-2765
DMSO
1μM
2μM
3μM
H3K27me3
H3
C
MSTC-2125
MSTC-2770
DMSO
1μM
2μM
3μM
H3K27me3
H3
D
MSTC-2125
Relative Invasion
Concentration (μM)
E
MSTC-2770
Relative Invasion
Concentration (μM)
F
MSTC-2125
MSTC-2770
MSTC-2549
MSTC-2765
Body Weight (grams)
Days (post injection)
Veh
MEKi
EZH2i
MEKi+EZH2i
G
MSTC-2549
MSTC-2765
Tumor Volume (mm³)
Veh
Vemurafenib
Vehicle
Vemurafenib
H
MSTC-2125
Number of VIM+ cells
p=0.015
p=2.864e-5
Vehicle
EZH2i
MEKi
MEK+ EZH2i
I
Vehicle
EZH2i
MEKi
EZH2i+MEKi
500 μm

Figure S6: Inhibition of EZH2 decreases invasion and tumor burden in NRAS -mutant melanoma. Related to Figure 6.

A-B) Western blotting for H3K27me3 in *BRAF*-mutant MSTC cell lines 2549 and B) 2765 treated for 14 days with GSK-126 or DMSO.

C) Western blotting for H3K27me3 in *NRAS*-mutant MSTC cell lines 2125 and 2770 treated for 14- or 10-days respectively with 3-Deazaneplanocin A (DZNep) or DMSO.

D-E) Boyden chamber invasion assay in *NRAS*-mutant MSTC cell lines 2125 and E) 2770 treated for 14- or 10- days respectively with 3-Deazaneplanocin A (DZNep) or DMSO. P-values were calculated using a t-test. * = $p < 0.05$; ** = $p = 0.001$. Error bars represent mean ± S.E.M.

F) Body weight of mice xenograft tumors from MSTC-2125, MSTC-2770, MSTC-2549 and MSTC-2765 treated with Vehicle, MEKi (Trametinib), EZH2i (GSK-126) or MEKi + EZH2i. P-values represent pairwise t-test comparison between the experimental arm to vehicle treatment. *** = $p < 0.001$. Error bars represent mean ± S.E.M.

G) Tumor volume curves for *BRAF*-mutant melanoma cultures MSTC-2549 and MSTC-2765 upon treatment with Vehicle and BRAF-inhibitor Vemurafenib (n = 4 for each arm). P-values represent pairwise t-test comparison between the experimental arm to vehicle treatment. *** = $p < 0.001$. Error bars represent mean ± S.E.M.

H) Barplot displaying the number of Vimentin positive cells from immunochemistry in MSTC-2125 mouse tumors treated with Vehicle, EZH2i, MEKi or EZH2i+MEKi. Cells were counted using imageJ based on a minimum of 9 20x images from each sample. P-values were calculated using a wilcoxon test.

I) Representative images from immunohistochemistry staining for Vimentin in MSTC-2125 mouse tumors treated with Vehicle, EZH2i, MEKi or EZH2i+MEKi. Scale bar represent 500μM.